

行政院國家科學委員會專題研究計畫 期中進度報告

穿越奈米孔洞高分子動態行為之研究(1/3)

計畫類別：個別型計畫

計畫編號：NSC91-2214-E-002-011-

執行期間：91年08月01日至92年07月31日

執行單位：國立臺灣大學化學工程學系暨研究所

計畫主持人：譚玉真

報告類型：精簡報告

處理方式：本計畫可公開查詢

中 華 民 國 92 年 5 月 21 日

The effect of topological constraint on the Theta temperature of a knotted polymer

計劃編號：NSC 91-2214-E-002-011

譚玉真*
臺灣大學化工系

Abstract

Monte Carlo simulations were used to study the effect of topological constraints of knotted polymers on their theta temperatures. The theta temperatures were determined through two different definitions - the vanishing of the second virial coefficient $A_2=0$, and the quasi-ideal behavior of the radius of gyration, $\langle Rg^2 \rangle \sim N$. Prime knots with chain lengths from $N=60$ to 300 and with crossings from 3_1 to 9_1 were considered. For chains with finite lengths, it was found that the theta temperature determined from quasi-ideal condition of the knot increases, as the complexity of the knot increases. On the other hand, the topological complexity seemed to have no effect on the theta temperatures determined from the vanishing of the second virial coefficient. Also, our simulation results suggest that for chains with finite crossing numbers, as $N \rightarrow \infty$, theta temperatures for all knots obtained from two different approaches coincide and are equivalent to that of a linear polymer chain.

Keywords: Monte Carlo simulation, second virial coefficient, topological constraint

一、Introduction

The theta point (θ) of macromolecules is traditionally viewed as the point at which excluded volume interactions exactly cancel the attractive interactions between monomers of the chain. Consequently, at the θ temperature chain dimension behave quasi-ideally, with the radius of gyration proportional to chain length, $\langle Rg^2 \rangle \sim N$. According to Flory's theory,¹ the theta temperature is also the point at which the polymer-polymer second virial coefficient vanishes. Bruns² has performed careful simulations on the 5-choice cubic lattice and has determined that the temperature for quasi-ideal chain dimensions coincides, within simulation uncertainty, with the temperature at which the second virial coefficient vanishes at the limit of long chains. Sheng et al.³ have extended the work to linear polymers in continuous space. It was found that the temperatures at which the second virial coefficients vanish are essentially constant for different chain length polymers and the estimated common value agrees, within simulation uncertainty, with the temperature at which an isolated polymer chain behaves as if it were a random coil (i.e. $\langle Rg^2 \rangle \sim N$).

Many biological macromolecules assume knotted forms. For example, DNA rings in bacteria take the form of a knotted ring, and there are certain types of enzymes that can act on circular DNA's and produce different types of DNA knots.^{4,6} The proteins, RNA's and DNA's are all polymers of biology origin. The physical properties of these molecules are strongly affected by their topological properties. Also, many molecular biological phenomena are associated with quite ordinary properties and characteristics of polymers. Thus studies of the physical properties of model knotted polymers can be of great help in understanding the basic physics of knotted type polymers and biopolymers.

Careful inspection reveals that due to the fundamental similarity in the topology of knots, conventional labeling of knots can further be classified naturally into groups, such as $(3_1, 5_1, 7_1, \dots)$, $(4_1, 6_1, 8_1, \dots)$ and $(5_1, 7_1, 9_1, \dots)$. The similarity in topological interactions in a group is also supported by the observation of the Alexander polynomials and Conway notations.^{7,8} Knots with only hard-core excluded volume

interactions and topological constraints, the nonequilibrium relaxation time of an equilibrated knot cut at one point to relax to a linear chain were found to increase stepwise linearly with number of essentially crossings of knots within a group.

Many other physical properties were also known to be affected by topological interactions. It was found that the average crossing number of flexible knotted polymer is consistent with a linear variation of the square root of the minimum crossing number, C .⁹ The effect of topological deformation on the mobility and diffusivity of a polymer chain was also investigated.¹⁰ The mobility declines as the crossing number of the knotted polymer increases. For a knotted polymer confined within a tube of diameter D , the equilibrium radius of gyration along the axial direction scales as $C^{-0.52} D^{-0.95}$ which has a stronger dependence on D than that of a linear chain. This indicates that the loops within a knot being forbidden to cross one another enhances the excluded interactions between the chain and the wall. In this work, we intend to perform an off-lattice Monte Carlo simulation to examine the effect of the topological interactions on a also very important physical quantity, the theta temperature of a knotted chain. The theta temperatures were determined through two different definitions-the vanishing of the second virial coefficient $A_2=0$, and the quasi-ideal behavior of the radius of gyration, $\langle Rg^2 \rangle \sim N$. The result can provide for us further understanding of knotted systems.

二、Simulation Details

The knotted polymer chain studied in this work is modeled as beads connected by springs. The interactions between the nonbonded beads are through the standard Square-Well potentials.

$$U_{nb} = \begin{cases} \infty, & r < t \\ -v, & t \leq r < \delta t \\ 0, & r \geq \delta t \end{cases} \quad (1)$$

where v and δ are the energy and size parameters, respectively and $\delta=1.5$. The monomeric v and δ are units used for the reduced quantities for temperature and distances as $T^*=kT/v$ and $R^*=R/\delta$. The interactions between bonded beads are represented by a infinite deep Square-Well potential as

$$U_b = \begin{cases} \infty, & r < t \\ 0, & t \leq r < gt \\ \infty, & r \geq gt \end{cases} \quad (2)$$

where $\delta=1.4$ is to prevent any bond crossing occurring within the knotted chain.

The systems studied contain a single polymer chain with chain length N ranging from 60 to 300. The simulations are performed under the conditions of constant temperature, volume and total number of beads. In the present study, the reduced temperature T^* is varied to study the system under different conditions. We have studied the knotted polymers up to ten crossings: $3_1, 4_1, 5_1, 5_2, 6_1, 7_1, 7_2, 8_1, 9_1, 9_2$. The standard notation for uniquely labeling a knot is C_K , where C is the number of essential crossings and K is an index for a particular

knot.^{11,12}

Figure 1(a) displays the schematic diagrams of some knots. The initial configurations of knots are generated by growing the chain bead by bead along the contour line of each knot to the desired length and knot type. For convenience, the knot is constructed on a lattice. The construction process is simple but tedious. Figure 1(b) and 1(c) show the top and side views of the constructed initial configuration of the 3_1 knot. From the top view, it is clear that there are three intersections indicating a knot with 3 crossings. At each intersection, one of the line goes under another line as can be seen in Figure 1(c). However, this procedure is nonrandom and must be proceeded according to the topological structure of the knot. Thus the topological constraint is conserved. Our previous works^{10,11} have successfully investigated the topological effects on properties such as relaxation time and diffusivity of knotted chains based on these initial configurations.

The trial moves employed for chains of the equilibration and production process are bead displacement motions which involve randomly picking a bead and displacing it to a new position in the vicinity of the old position. The distance away from the original position is chosen with probability that the condition of equal sampling of all points in the spherical shell surrounding the initial position must be satisfied. The new configurations resulting from this move are accepted according to the standard Metropolis acceptance criterion.¹³ Runs for the same chain length at different temperatures are performed starting with the final configuration from a previous temperature and are equilibrated for 200 million steps. Measurements for static properties such as radius of gyration are taken over a period of 5-10 millions MCS/monomer.

The root-mean-squared radius of gyration of isolated polymer chains was determined by

$$\langle R_g^2 \rangle^{1/2} = \left\langle \frac{\sum [(x_i - x_{cm})^2 + (y_i - y_{cm})^2 + (z_i - z_{cm})^2]}{N} \right\rangle^{1/2} \quad (3)$$

where (x_i, y_i, z_i) are the coordinates of the i th monomer in the chain and (x_{cm}, y_{cm}, z_{cm}) are the coordinates of the center of mass of the chain. The angular brackets $\langle \dots \rangle$ denote ensemble average.

The virial expansion for the compressibility factor takes the form¹⁴

$$SP/\dots = 1 + A_2\dots + A_3\dots^2 + \dots, \quad (4)$$

where P is the pressure, \bar{n} is the molecular number density of the system, A_2, A_3 are the second and third virial coefficients, respectively, $\hat{\alpha}=1/kT$, k is the Boltzmann's constant and T is the temperature. To calculate the second virial coefficient, we used the algorithm proposed by Harismiadis and Szleifer.¹⁵ The second virial coefficient can be calculated in terms of the interaction potentials from standard statistical mechanics^{16,17}

$$A_2 = 2\mathcal{f} \int \left[1 - \exp\left[-\frac{F_2(\hat{\alpha}) - 2F_1}{kT} \right] \right] k^2 d\hat{\alpha}, \quad (5)$$

where F_1 is the Helmholtz free energy of a single chain at infinite dilution in a solvent, and $F_2(\hat{\alpha})$ is the Helmholtz free energy of a system composed of the same solvent and two polymer molecules when their center of mass distance is $\hat{\alpha}$. The difference in the exponential can be thought of as an effective potential between the chain molecules, i.e.

$$U_{eff}(\hat{\alpha}) = F_2(\hat{\alpha}) - 2F_1 = -kT \ln \langle \exp[-SU_{inter}(\hat{\alpha})] \rangle \quad (6)$$

where U_{inter} is the intermolecular interaction energy between the two polymer molecules. $\langle \dots \rangle$ denotes a canonical average over all the configurations of the two chains however each chain does not know the presence of the other chain. If there are no overlaps, it equals to the number of segment pairs belonging to the two interacting polymers with distance lying between $\hat{\alpha}$ and $1.5\hat{\alpha}$,

multiplied by the well depth. A trial move leading to overlap of two knots is allowed but yields an infinite value of intermolecular interaction, U_{inter} . The typical example is the A_2 calculation for two hard-spheres of radius R . When the distance between the two particles is less than $2R$, i.e. $\hat{\alpha} < 2R$, all sampling by rotations result in $U_{eff}(\hat{\alpha}) = \infty$. As a consequence, one obtains the theoretical value $A_2 = 16\delta R^3/3$ from MC simulations.

The algorithm used to calculate U_{eff} and then A_2 is as follows: 200,000 completely independent chain conformations are generated by using the Metropolis recipe.¹³ A pair of chains is selected out of 100,000 pairs. One of the pair is placed with its center of mass fixed at $(0, 0, 0)$. Then place another chain with its center of mass set at $(\hat{\alpha}, 0, 0)$, i.e. two chains are separated by a distance of $\hat{\alpha}$ and $\hat{\alpha}$ is systematically increased during the simulation process to estimate the U_{eff} at different separations. At each separation, 50 random rotations of the second chain are performed. A total of 5,000,000 U_{inter} are sampled at each separation. After the effective potential between the chains is calculated (eq.(6)) as a function of $\hat{\alpha}$, the second virial coefficient can be obtained through eq.(5). Similar procedures have already been used in various studies.¹⁵⁻²¹

Note that the approach adopted in our simulations for A_2 calculations cannot preclude the formations of concatenated knots as two knotted chains are close to each other. In principle, they can be avoided through time-consuming, elaborated simulation procedures. However, it is believed that the probability of the formation of concatenated knots is very small as will be discussed later. Our present approach provides accurate results and yet is time-saving.

Ξ 、 Results and Discussion

Figure 2 shows the calculated second virial coefficients A_2 of 3_1 knot as a function of temperature for a variety of chain lengths ranging from 60 to 120 monomers per chain. The qualitative behavior of the virial coefficient with temperature of a knotted polymer is the same with its linear counterpart. At low temperatures, the attractive interactions dominate and A_2 is negative. A_2 increases as the temperature increases. There exists a temperature (that is, the theta temperature) where the attractive and the repulsive intermolecular interactions exactly cancel and thus the second virial coefficient vanishes. For a 3_1 knot, the θ temperature is found to be around $T^* = 2.55$. It has been well known that the theta temperature obtained from the vanishing second virial coefficient definition is a fairly weak function of chain length.^{2,3,15,22} The θ temperature obtained for short-length chain is very close to the true theta temperature. Below the θ temperature, the solvent is poor. The longer the chain length is the more negative the second virial coefficient is. On the other hand, above the θ temperature, the solvent becomes good. The chains are in expanded conformations and for two chains of distance $\hat{\alpha}$ apart, the chance of overlapping between segments increases. The chance of overlapping also increases as chain length increases. Thus, A_2 for longer chain becomes more positive than that of the shorter chain. This result is consistent with the fact that in a good solvent, the second virial coefficient is proportional to the excluded volume of the chain which increases with increasing chain length.

We have also performed simulations for linear polymer chains as displayed in Figure 3. The behavior are qualitatively similar to that of the knotted polymer. The estimated theta temperature for linear chain is about 2.56. The second virial coefficients for polymers of length $N=60$ but with different topological structures are plotted as a function of temperature in Figure 4. Although the absolute values of A_2 for linear chain vary more significantly than the knotted counterparts, the general behaviors for linear and knotted polymers are actually quite similar. Table 1 lists the values of the calculated theta temperatures of different knots for chain length $N=90$. From the Table, it can be seen that the topological complexity seemed to

have no effect on the theta temperatures determined from the second virial coefficient approach. The θ temperature are essentially the same (within simulation errors) for different knot types we have studied. This result again shows that the topological constraint has almost no effect on the theta temperature estimated from vanishing of A_2 .

In the experimental works of Roovers et al.,^{23,24} some physical properties, such as the theta point, of both linear and ring polymers of the same molecular weight are studied. They found that the theta temperature is essentially independent of molecular weight which is consistent with our finding. However, they found slight (about 2%) theta point depression for the ring polymer. As listed in Table 1 of our manuscript, varying degrees of theta point depression (up to 3%) are also observed for the knotted type polymers. From our previous works,^{10,11} we found that topological effects have significant effect on some of the physical properties, such as radius of gyration, relaxation time and diffusivity. However, the degrees of the theta point depression resulted in this work seem to be quite insignificant. Thus, we concluded the independence of the theta temperature on topology. It is worth mentioning that this study provides the leading behavior and a realistic potential model may be needed to probe the slight difference in theta temperature change.

It is also possible for us to use the calculated effective potentials to demonstrate the radial distribution function, $g(\hat{r})$ as a function of the distance \hat{r} ,

$$g(\hat{r}) = \exp[-U_{\text{eff}}/kT] \quad (7)$$

Figure 5 shows the radial distribution function as a function of the distance between centers of mass for linear-linear, 3_1 knot- 3_1 knot, 6_1 knot- 6_1 knot and 9_1 knot- 9_1 knot pairs for $N=60$ and $T^*=2.6$. As we can see from the figure, $g(\hat{r})$ behaves differently for linear-linear and knot-knot pairs. For two linear polymers, penetration between them is more probable than that of knotted polymers. That is, the two linear polymers can relatively easily penetrate into each other. However, knotted polymers are of ring structure. The radius of gyration of knotted polymers are significantly smaller than that of a linear chain with the same length. Thus the monomer density of a knotted chain is greater than the monomer density of a linear chain. The penetration of knotted chains into each other is relatively more difficult in close distance.

Also, as we have mentioned earlier, it is believed that the formation of the concatenated knot is possible but with slim chance. Since bond crossing is forbidden for non-phantom knots, the concatenated knot formation should correspond to an infinite value of intermolecular interaction, U_{inter} . In our calculation, however, the concatenated knot formation would result in a finite value of U_{inter} . If such events take place frequently, the A_2 value calculated in our work would be lower than its actual value. However, as we can see from Fig. 5, as \hat{r} is approximately less than $2R_g$, $g(\hat{r}) = \exp[-U_{\text{eff}}/kT] > 0$, which means $U_{\text{eff}} < 0$. This result indicates that in the regime where concatenated knots can possibly form, the effective hard-sphere behavior dominates. This implies that the chance of concatenated knots formation is slim and can be neglected. Note that for a linear chain, the effective hard-sphere behavior is not as significant. It is because knotted polymers have higher intrachain monomer density. When two knots are placed in close proximity, there is a greater possibility that they will overlap instead of forming concatenated knots.

Also, the linear polymer pairs have long-ranged repulsive interactions. However, for knotted chain pairs, attractive interactions at distances between 5 and 10 times the segment diameter can be clearly seen in Fig. 5. Also, as we know, R_g of knots scales as $C^{-4/15}$. Thus as the complexity of knot increases, R_g decreases accordingly. The distance where maximum attractive interaction occurs between two knots becomes less for more complex knots.

As we have mentioned earlier, the θ point can also be the temperature at which the excluded volume interactions exactly cancel the attractive interactions between monomers of the chain and $\langle R_g^2 \rangle^{1/2} \sim N^{1/2}$. However, for knotted polymer, the intrachain interactions also include the topological contribution which does not exist in a linear chain. R_g is not only the function of chain length but also affected by the complexity of the knot. Thus, we have performed simulations to study the effect. Figures 6 and 7 are $\langle R_g^2 \rangle^{1/2}/N^{1/2}$ vs. T for linear and 6_1 type knotted polymers. If $\langle R_g^2 \rangle^{1/2}$ is proportional to $N^{1/2}$ at some value of T , the curves belonging to all chain lengths N will intersect at a single point. As shown in Figure 6, the variations of R_g versus temperature of linear chains are quite sharp and all the curves seem to intersect at a single point. However, Figure 7 shows the variations of R_g versus temperature of 6_1 knot. For the chain lengths we have studied, the curves do not intersect at a single point, even for the longest chains. The temperature at which two chain lengths intersect increases with chain length. These observations are in agreement with the results of previous studies^{2,3}. The values of the estimated intersection temperatures obtained from the radius of gyration calculations for chain length up to $N=120$ are 2.27, 2.33, 2.36 and 2.44 for linear, 3_1 , 6_1 and 9_1 knot chains, respectively. These results are obtained for chains with finite length. For chains with even longer length, the intersection temperature continues to slowly rise. However, for knots with equal length, noted that the theta temperatures appear to be increasing as the complexity of the knotted polymer increases. This is because for knots with more crossings, they have more compact structures due to topological constraints. Thus, the exact cancellation of the attractive and repulsive interactions can only be achieved at higher temperature. For knots with finite crossing numbers, the topological effects will become less and less important as chain length increases. It is known that for a linear long chain, the probability for it to assume open knotted formation grows exponentially with N . In other words, the entropy-induced, self-knotted structures are formed naturally for all types of chains. The extrapolation of the intersection temperatures to chains of infinite chain length are believed to be the same for all the knots and linear chains we have studied. Also in the infinite chain length regime, N temperatures determined through two different definitions - the vanishing of the second virial coefficient $A_2=0$, and the quasi-ideal behavior of the radius of gyration, $\langle R_g^2 \rangle \sim N$ are expected to coincide into a single value.

四、References

1. P.J. Flory, Cornell University Press: Ithaca, NY (1953).
2. W. Bruns, *Macromolecules* 17, 2826 (1984).
3. Y.-J. Sheng, A. Z. Panagiotopoulos, S. K. Kumar and I. Szleifer, *Macromolecules* 27, 400 (1994).
4. W. R. Bauer, F.H.C. Crick, and J. H. White, *Sci. Am.* 243, 118 (1980).
5. N. R. Cozzarelli, S.J. Spengler, and A. Stasiak, *Cell* 42, 325 (1985).
6. S.A. Wasserman and N. R. Cozzarelli, *Science* 232, 951 (1986).
7. G. Burde and H. Zieschang, *Knots* (Walter de Gruyter, Berlin, 1985).
8. C. C. Adams, *The Knot Book* (Freeman, New York, 1994).
9. J.-Y. Huang, Ph.D. thesis of the Department of Physics, National Central University (2002).
10. Y.-J. Sheng and H.-K. Tsao, *J. Chem. Phys.* 116, 10523 (2002).
11. Y.-J. Sheng, P.-Y. Lai, and H.-K. Tsao, *Phys. Rev. E.* 58, R1222 (1998).
12. G. Burde, H. Zieschang, *Knots*, Walter de Gruyter, Berlin, 1985.
13. M. P. Allen and D. J. Tildesley, *Computer Simulations of Liquids*, Oxford University Press: New York (1987).
14. C. G. Gray and K. E. Gubbins, *Theory of Molecular*

Fluids; Clarendon Press: Oxford, UK, 1982.

15. V. I. Harismiadis and I. Szleifer, *Molecular Physics* 81, 851 (1994).
16. D. A. McQuarrie, *Statistical Thermodynamics* (New York: Harper & Row), 1976.
17. H. Yamakawa, *Modern Theory of Polymer Solutions*; Harper and Row: New York, 1971.
18. J. Dautenhahn and C. K. Hall, *Macromolecules* 27, 5399 (1994).
19. A. Yethiraj, K. G. Honnell and C. K. Hall,

Macromolecules 25, 3979 (1992).

20. L. Lue and J. M. Prausnitz, *AIChE J.* 44, 1455 (1998).
21. A. Striolo and J. M. Prausnitz, *J. Chem. Phys.* 113, 2927 (2000).
22. M. Janssens and A. Bellemans, *Macromolecules* 9, 303 (1976).
23. J. Roovers and P. M. Toporowski, *Macromolecules* 16, 843 (1983).
24. J. Roovers, *J. Polym. Science, Polym. Phys. Ed.* 23, 1117 (1985).

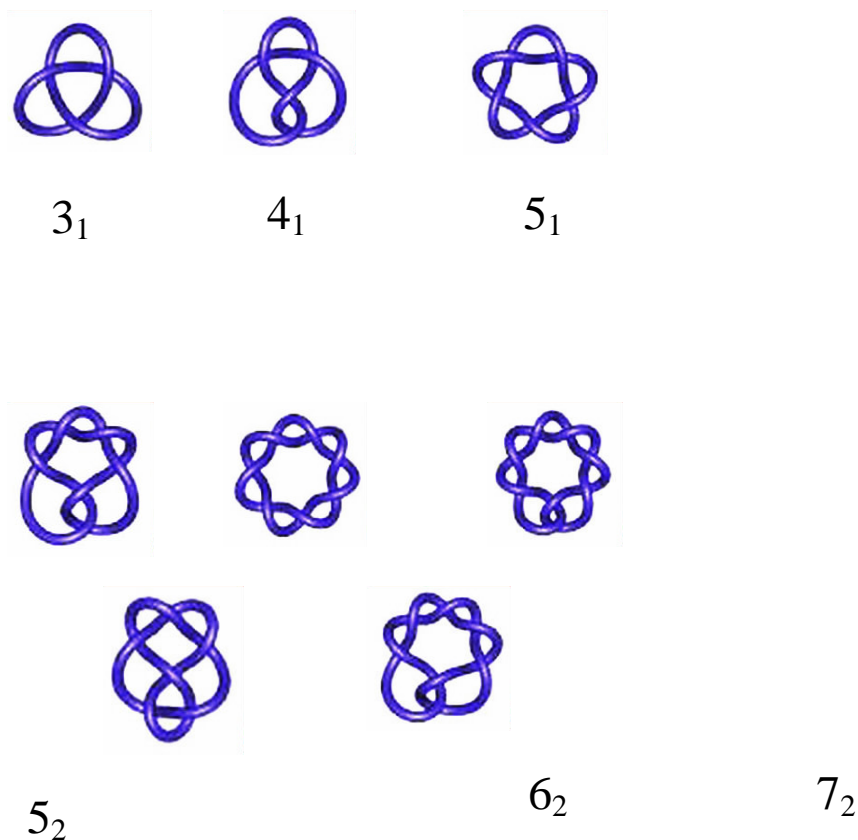
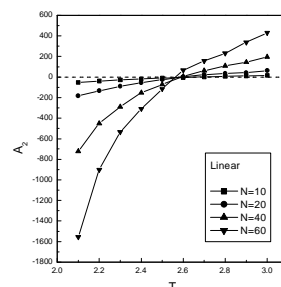
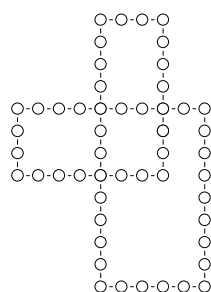
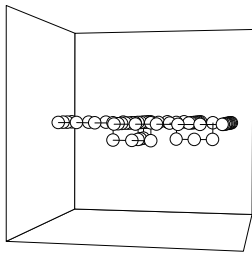


Figure 1(a). Schematic knot diagrams. The conventional nomenclature of a knot is denoted by $C_{\{K\}}$ where C is the number of essential crossings and K is a label to distinguish topologically different knots.



(b) The top view of the constructed initial configuration of the 3_1 knot.



(c) The side view of the constructed initial configuration of the 3_1 knot.

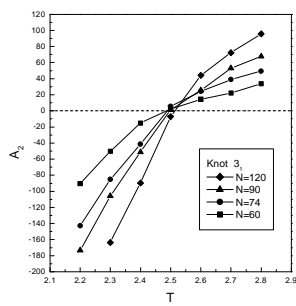


Figure 2. Calculated second virial coefficients A_2 of 3_1 knot as a function of temperature for a variety of chain lengths ranging from 60 to 120 monomers per chain.

Figure 3. Calculated second virial coefficients A_2 of a linear polymer as a function of temperature for a variety of chain lengths ranging from 10 to 60 monomers per chain.

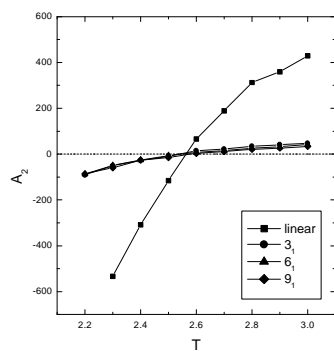


Figure 4. Calculated second virial coefficients A_2 as a function of temperature for different types of chains with length equal to 60 monomers per chain.

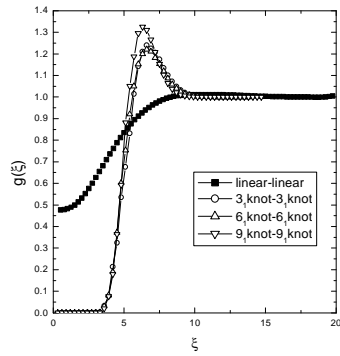


Figure 5. The radial distribution function as a function of the distance between centers of mass for linear-linear, 3_1 knot- 3_1 knot, 6_1 knot- 6_1 knot and 9_1 knot- 9_1 knot pairs for $N=60$ and $T^*=2.6$.

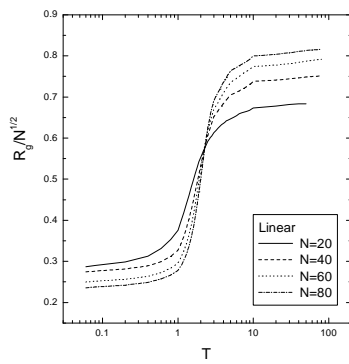


Figure 6. The radius of gyration, $\langle R_g^2 \rangle^{1/2}/N^{1/2}$ as a function of the temperature for linear polymers of lengths equal to $N=20-80$.

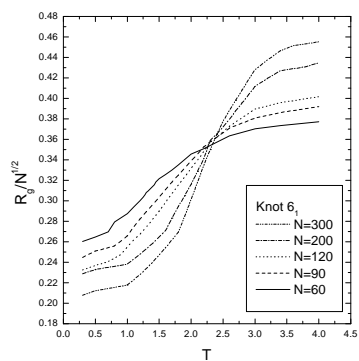


Figure 7. The radius of gyration, $\langle Rg^2 \rangle^{1/2}/N^{1/2}$ as a function of the temperature for 6 knot polymers of lengths equal to $N=60-300$.

Knot type	θ temperature
3 ₁	2.55
4 ₁	2.55
5 ₁	2.49
5 ₂	2.54
6 ₁	2.53
7 ₁	2.51
7 ₂	2.54
8 ₁	2.56
9 ₁	2.55
9 ₂	2.54

Table 1. Calculated theta temperatures of different knots with chain length $N=90$ from the vanishing second virial coefficient definition. The estimated theta temperature for linear chain is about 2.56.